Research Paper
J. Astron. Space Sci. 34(3), 199-205 (2017)
https://doi.org/10.5140/JASS.2017.34.3.199

JASS Journal of Astronomy and Space Sciences

Chemical Composition of RM_1-390 - Large Magellanic Cloud Red Supergiant

Alexander V. Yushchenko[1], Yeuncheol Jeong[1†], Vira F. Gopka[2], Svetlana V. Vasil'eva[2], Sergey M. Andrievsky[2,3], Volodymyr O. Yushchenko[2]

[1]Sejong University, Seoul 05006, Korea
[2]Astronomical observatory, Odessa National University, Odessa 65014, Ukraine
[3]GEPI, Observatoire de Paris, PSL Research University, CNRS, Place Jules Janssen, 92195 Meudon, France

A high resolution spectroscopic observation of the red supergiant star RM_1-390 in the Large Magellanic Cloud was made from a 3.6 m telescope at the European Southern Observatory. Spectral resolving power was R=20,000, with a signal-to-noise ratio S/N > 100. We found the atmospheric parameters of RM_1-390 to be as follows: the effective temperature T_{eff} = 4,250 ± 50 K, the surface gravity log g = 0.16 ± 0.1, the microturbulent velocity v_{micro} = 2.5 km/s, the macroturbulence velocity v_{macro} = 9 km/s and the iron abundance [Fe/H] = -0.73 ± 0.11. The abundances of 18 chemical elements from silicon to thorium in the atmosphere of RM_1-390 were found using the spectrum synthesis method. The relative deficiencies of all elements are close to that of iron. The fit of abundance pattern by the solar system distribution of r- and s-element isotopes shows the importance of the s-process. The plot of relative abundances as a function of second ionization potentials of corresponding chemical elements allows us to find a possibility of convective energy transport in the photosphere of RM_1-390.

Keywords: supergiants (RM_1-390), individual (RM_1-390), abundances, accretion, chemically peculiar, individual (Large Magellanic Cloud)

1. INTRODUCTION

The Magellanic Clouds and our galaxy are members of the Local Group. Tidal interactions between the Large and Small Magellanic Clouds (LMC and SMC) and the Milky Way produce several high-velocity gas complexes connecting all three galaxies. The Magellanic Clouds appear to be optimal targets for investigations into stellar formation history in the Local Group. They have often been used to test the validity of galactic evolution theories. The high resolution spectroscopic observations of the brightest stars of these galaxies became available. As a rule, many spectroscopic analyses of the LMC/SMC supergiants only focused on the determination of elemental abundances for atomic numbers Z ≤ 64. Apparent progress achieved recently in the field of quantitative and experimental spectroscopy together with a continued improvement of the numerical codes used for the abundance analysis, made it possible to detect heavy elements in their stellar atmospheres such as, uranium and thorium.

These elements are produced in the universe as a result of neutron-capture processes; the so-called s- and r-processes of nucleosynthesis. Among other factors, the yield of these neutron-capture elements may depend upon the overall metallicity of the progenitor star. It is well known that the metal content of the Magellanic Clouds is lower than that of our galaxy. This leads to an investigation on specific conditions of their chemical evolution that is reflected in the peculiar elemental distribution observed in their stellar population.

Note that the final evolutionary stage of red supergiants was usually discussed as a supernova outburst. Recently (Kochanek et al. 2008; Adams et al. 2017a, b), it was found that a significant fraction of red supergiants, namely 0.04-0.47 (with the most reliable fraction near 0.14) can disappear

Received 15 AUG 2017 **Revised** 30 AUG 2017 **Accepted** 31 AUG 2017
†**Corresponding Author**
Tel: +82-10-5679-3177, E-mail: yeuncheoljeong@sejong.ac.kr
ORCID: https://orcid.org/0000-0001-5775-4610

without explosion; the core collapse of a massive star decreases the brightness of an initial source below the detection limit. This observational result shows the necessity of investigations into the individual supernova progenitors to separate criteria for outbursts, or shows that the core collapse evolutionary path is not yet clearly understood.

In this paper, we derive the elemental abundances in LMC supergiant star RM_1-390, with an emphasis on a detailed investigation into the s- and r-process elemental abundances. We determined the abundances of 19 elements in the atmosphere of RM_1-390 and compared its abundance pattern to other LMC and SMC supergiants.

2. SPECTROSCOPIC OBSERVATIONS AND ATMOSPHERIC PARAMETERS

The high resolution spectral observation of RM_1-390 was obtained from the 3.6 m telescope at the European Southern Observatory by Hill (1997). The spectrum was obtained by V. Hill, but was not used in her publications. This paper is the first to determine the abundance pattern for RM_1-390. The signal-to-noise ratio (S/N) of the spectrum is greater than 100 (S/N > 100) while the resolving power was equal to R = 20,000 and the wavelength coverage is from 5,850 Å to 7,095 Å with several gaps between orders. The extraction of the observed spectrum from charge-coupled device (CCD) imaging and its wavelength calibration were made by Hill (1997). The next reduction steps are the determination of the continuum level and then the identification of spectral lines made with URAN (Yushchenko 1998) and SYNTHE (Kurucz 1993) codes. Fig. 1 shows an example of the observed spectrum.

The list of atomic and molecular lines was taken from Kurucz (1993), Hirata & Horaguchi (1995), Morton (2000), DREAM data base (Biémont et al. 2017), VALD data base (Piskunov et al. 1995), Fuhr & Wises (2006) and other sources. The clean and not strongly blended lines in the observed spectrum were selected on the basis of comparison with the synthetic spectrum. The detailed calculation procedure can be found in Yushchenko et al. (2015) and Kang et al. (2013).

The effective temperature, surface gravity and other stellar parameters were found using the method, developed by Yushchenko et al. (1999) and Gopka et al. (2004). This method uses the iron abundances calculated from various spectral lines under the different stellar atmosphere models to determine the stellar parameters. The grids of the atmosphere models with effective temperatures from 3,900 K to 4,500 K (step 10 K) and surface gravities from log(g)=0.00 to 0.50 (step 0.02) were prepared by the interpolations of Kurucz (1993) atmosphere models. Afterwards, the following parameters were derived: the effective temperature T_{eff} = 4,250 ± 50, the surface gravity log g = 0.16 ± 0.1, the microturbulent velocity v_{micro} = 2.5 ± 0.1 km/s, and the iron abundances [Fe/H] = -0.73 ± 0.11. Thirty-nine lines of neutral iron and 10 lines of ionized iron were used for these calculations. The errors pointed out are estimated from the errors of the used method. The level of the systematic errors can be higher, as illustrated in Table 1.

Table 1 shows the spectral types, colors and radial velocities of the Magellanic Clouds red supergiants observed by Hill (1997). Their temperatures are taken from Massey & Olsen (2003) for RM_1-390, from Gopka et al. (2012a) for RM_1-667, and from Hill (1997) for the rest of the stars. The references for their spectral types and colors are included in the table. Their published radial velocities, and the minimum and maximum values with the differences between these extrema are taken from the SIMBAD data base.

The temperature of RM_1-390 was found to be 3,200 K by Massey & Olsen (2003). This value is a thousand degrees lower than our determination and needs to be discussed. It is to be noted that B-V color for PMMR144 and U-B colors for RM_1-390 and RM_1-667 are not usual for late type stars. One of the possible explanations for these can be the existence of a close blue companion; a member of binary system or a background/foreground star. In the case of a binary system, the variations of radial velocities should be observed. Two of the aforementioned three stars, namely PMMR144 and RM_1-390, exhibit the greatest differences

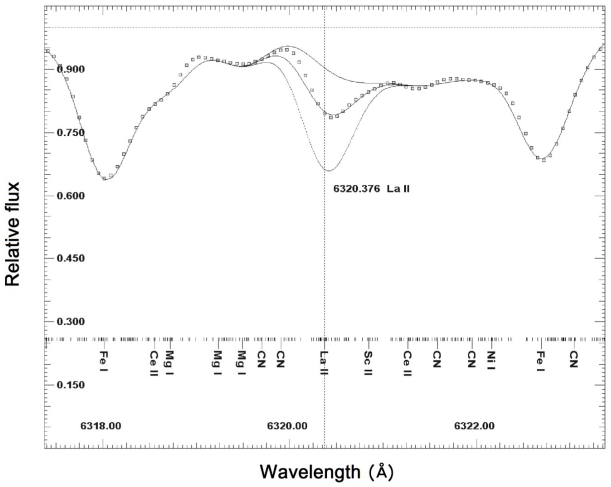

Fig. 1. The example of RM_1-390 spectrum. The axes are wavelength and relative flux. The open squares denote the observed spectrum, the lines – synthetic spectra. The positions of the spectral lines, which were taken into account in the calculations, are marked in the bottom part of the figure by short and long dashes (faint and strong lines, respectively). The identifications are shown for the strongest lines. Three synthetic spectra in the vicinity of lanthanum line were calculated with the best abundance of this element, with the abundances increased and decreased by 0.5 dex.

Table 1. The temperatures, spectral types, colors and radial velocities of several red supergiants in the Magellanic Clouds

Star	Teff	Spectral type	Ref.	B-V	U-B	Ref.	N_{Vr}	Vr (min-max)	ΔVr
RM_1-390	3200	M3I	2	1.52	0.23	7	3	270.2-282.7	12.5
RM_1-667	4100	K7I	2	1.50	0.30	7	3	293.8-298.6	4.8
PMMR23	4200	K5-M0Iab	1	1.76	1.37	5,6	4	140.4-147.7	7.3
PMMR27	4300	K1Ia-Iab	3	1.77		2	3	161.5-164.8	3.5
PMMR48	4300	K5-M0I	4	1.79	1.69	6	5	157.1-167.7	10.6
PMMR102	4300	G7.5Ia-Iab	3	1.72	1.50	6	4	155.0-162.1	7.1
PMMR144	4100	K3-5I	2	1.12		8,7	6	151-189.9	38.9

References: 1 Humphreys (1979), 2 Massey & Olsen (2003), 3 González-Fernández et al. (2015), 4 Elias (1985), 5 Bonanos et al. (2010), 6 Boyer et al. (2011), 7 Bonanos et al. (2009), 8 Munari et al. (2014)

between the minimum and maximum published radial velocities, 38.9 and 12.5 km/s, respectively. We can conclude that the low effective temperature value for RM_1-390, published by Massey & Olsen (2003), can be explained by an unresolved binary companion. The case of real physical variations is also possible; Szczygieł et al. (2010), found the brightness varies between V = 12.2 to 12.7 at the time scale near ten years and nearly one year with an amplitude of almost 0.1 magnitude. Our set of parameters found for the moment of the spectral observation was used to derive the chemical composition of RM_1-390.

The abundances of all chemical elements except for iron were found using the spectrum synthesis method. It requires additional information to take into account the broadening effect of the spectral lines. It was assumed that the broadening is due to the macroturbulence in the atmosphere of RM_1-390. The value of the macroturbulence velocity was found by fitting the profiles of clean lines of neutral iron to the synthetic profiles, calculated with different values of the macroturbulence velocity. The best fit was found for the value, $v_{macro} = 9$ km/s.

3. CHEMICAL COMPOSITION

To derive the elemental abundance in our program stars, we used the synthetic spectrum technique. The synthetic spectra were generated using Kurucz's (1993) code, SYNTHE. The fit of the observed spectrum with the synthetic one was made with the URAN code (Yushchenko 1998). Hyperfine and isotopic splitting are taken into account for some elements such as Mn, Co, Ba, and Eu, using the data (mainly) from Kurucz (1993). To avoid some possible errors in the oscillator strengths, we tried to find the counterparts of investigated absorption lines in the solar spectrum. The Liege Solar Atlas (Delbouille et al. 1973) and the Grevesse & Sauval (1999) solar photosphere model were used to find the abundances in the solar atmosphere. The continuum in the Liege Solar atlas was corrected in accordance with the works of Ardeberg & Virdefors (1979) and Rutten & van der Zalm (1984). A more detailed description of the method can be found in Yushchenko et al. (2015), and Kang et al. (2013).

Table 2. Chemical composition of RM_1-390 (with respect to the Sun)

Z	Elem.		n	ΔlogN	log(g+0.2)	T_{eff}+100 K	Marcs
14	Si	I	2	-0.88(10)	-0.85(10)	-0.87(10)	-0.85(09)
20	Ca	I	8	-1.06(23)	-1.06(27)	-0.98(19)	-1.06(30)
22	Ti	I	8	-0.59(14)	-0.61(14)	-0.51(23)	-0.61(18)
		II	1	-0.95	-0.86	-1.01	-0.97
23	V	II	3	-0.69(01)	-0.68(00)	-0.61(10)	-0.70(01)
		II	2	-0.54(02)	-0.57(05)	-0.53(05)	-0.57(01)
25	Mn	I	2	-0.82(11)	-0.80(09)	-0.69(12)	-0.71(14)
27	Co	I	1	-0.52	-0.49	-0.39	-0.51
28	Ni	I	1	-0.88	-0.84	-0.74	-0.74
39	Y	II	2	-0.72(17)	-0.71(17)	-0.38(14)	-0.71(15)
		II	1	-0.51	-0.47	-0.51	-0.67
40	Zr	II	2	-0.72(11)	-0.72(14)	-0.57(26)	-0.61(25)
56	Ba	II	2	-0.72(10)	-0.67(05)	-0.76(01)	-0.48(18)
57	La	II	7	-0.53(12)	-0.55(14)	-0.53(11)	-0.52(14)
58	Ce	II	6	-0.51(23)	-0.66(22)	-0.56(26)	-0.46(26)
59	Pr	II	6	-0.72(03)	-0.71(02)	-0.71(02)	-0.71(02)
60	Nd	II	16	-0.65(08)	-0.65(09)	-0.66(08)	-0.64(12)
62	Sm	II	2	-0.68(02)	-0.68(02)	-0.68(02)	-0.68(01)
63	Eu	II	2	-0.25(06)	-0.21(10)	-0.25(06)	-0.44(12)
64	Gd	II	2	-0.70(00)	-0.66(00)	-0.58(11)	-0.68(02)
90	Th	II	1	-0.71	-0.69	-0.71	-0.71

Based on the LTE approximation, both the plane-parallel (Kurucz 1993) and the spherically symmetric (Gustafsson et al. 2003) atmosphere models were used. The fit of the observed spectrum by the synthetic one in the vicinity of lanthanum line is shown in Fig. 1.

Table 2 summarizes the abundance calculations. The first three columns of the table are the atomic number, the designation of each chemical element with its ionization and the number of used spectral lines. In columns four through seven, one can find the mean chemical abundances in the atmosphere of RM_1-390 with respect to the solar photosphere abundances. The last figures in parenthesis after the corresponding relative abundances show the calculated errors. Four atmosphere models were used, one model for the stellar parameters, described in the previous section, another one for the surface gravity increased by

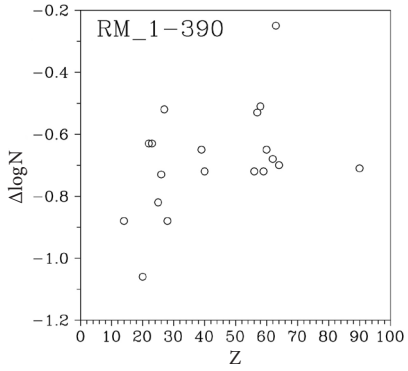

Fig. 2. Chemical composition of RM_1-390. The axes are the atomic numbers of chemical elements and the logarithmic abundances with respect to solar values. The horizontal dashed line marks the solar abundances and open circles designate the abundances in the photosphere of primary companion while filled circles denote the secondary one.

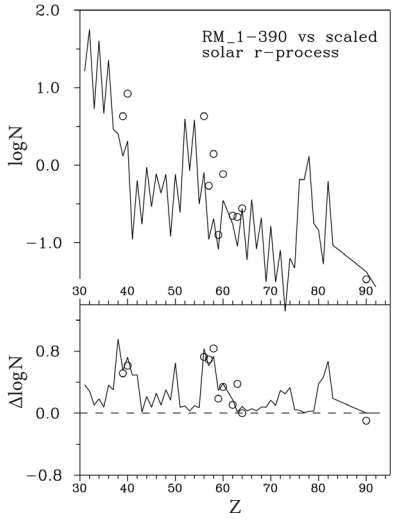

Fig. 3. Upper panel: the comparison of the surface abundances in RM_1-667 (circles) with the solar system r-process abundance distribution (Simmerer et al. 2004) scaled at the observed Gd abundance (line). Bottom panel: the differences of observed abundances in RM_1-667 and scaled solar system r-process abundances (circles). The line is the deviation of solar photosphere abundances from the solar r-process abundance distribution. The maxima of this curve are expected for the elements with the highest relative s-process contributions.

0.2 dex, another one for the effective temperature increased by 100 K and the last model from the MARCS grid (Gustafsson et al. 2003).

The abundances of 18 chemical elements from silicon to thorium were found in the atmosphere of RM_1-390 from the model synthesis. Fig. 2 shows the abundance patterns of RM_1-390.

4. DISCUSSION

All chemical elements in the atmosphere of RM_1-390 show the underabundances with respect to the solar values. The values of underabundances are close to -0.7 dex; the iron deficiency in the atmosphere of this star. It is not a surprising result given that the deficiency of chemical elements in the Large Magellanic Cloud is a well-known fact, the mean metallicity of LMC is [Fe/H] = -0.37 ± 0.12 (Choudhury et al. 2016). The distribution of individual chemical elements in the abundance patterns of the various LMC stars is more interesting. Fig. 2 shows that the lowest relative abundance is observed for calcium while the highest is observed for europium. The europium and other neutron capture elements will be discussed next.

Fig. 3 compares the abundances of the r- and s-process elements in the atmosphere of RM_1-390 with the solar system distributions of these elements. This allows us to claim that the r-process elements in the atmosphere of RM_1-390 exist, but the role of the s-process is more important than in other Magellanic Clouds red supergiants. For example, we can point out the investigation by Gopka et al. (2013b), where the abundance patterns of PMMR23, PMMR144, and RM_1-667 were found, and also another by Gopka et al. (2012b, 2013a) where the absorption lines of osmium and thorium were found in the spectra of several other red supergiants; PMMR23, PMMR144, and RM_1-667 exhibit the excess of the r-process elements.

RM_1-390 is the first star in our sample without the overabundances of the r-process elements with respect to iron. It should be noted that the r-process elements lines can be detected. As an example of this, we can point to two thorium lines in the spectrum of RM_1-390, identified by Gopka et al. (2013a), and europium and gadolinium lines in this study, but the deficiencies of thorium and gadolinium are close to that of iron.

It is necessary to note that RM_1-390 is one of the strongest infrared objects in the LMC. It is detected at a wavelength as long as 24 microns (Bonanos et al. 2009) and the significant infrared excess is observed at wavelengths longer than 8 microns. That is why it is possible to expect the existence of the circumstellar envelope. To detect the possible signs of this envelope, we plot the dependencies of the relative surface abundances in the atmosphere of RM_1-390 as a function of the second ionization potentials (Fig. 4) of the corresponding chemical elements.

The most interesting feature of Fig. 4 is the deficiency of calcium. It was first pointed by Greenstein (1949) and can be explained by the charge-exchange reactions of calcium and hydrogen atoms. Unfortunately, this hypothesis is not fully developed yet. Recently, Yushchenko et al. (2015) made a review devoted to this problem, and found some new possible observational confirmations. One of them is the correlation

between relative surface abundances and the second ionization potentials in the range from 12.5 to 20 eV for the groups of stars with different effective temperatures. As shown by Yushchenko et al. (2015, Fig. 7), this correlation is positive for the groups of stars with effective temperatures in the range of 7,000-12,000 K, and negative for groups of stars with lower temperatures, specifically in the 5,900-7,000 K range. Maybe it can be explained by the transition from radiative to convective atmospheres. Our preliminary results show a positive correlation for red giant stars, where the radiative energy transfer becomes significant again.

We found the abundances of eight chemical elements with their second ionization potentials from 12.5 to 20 eV in the atmosphere of RM_1-390. The correlation coefficient between the abundances and the second ionization potential is negative, specifically ρ = -0.33 ± 0.32. The value of the error is defined mainly from the case of cobalt, which has the highest relative abundance in this range of potentials. It should be noted that the abundance of cobalt was determined by only one line. The relative abundance of cobalt in the surveys used by Yushchenko et al. (2015) was also higher than the relative abundances of other chemical elements in this range of the second ionization potentials. Without cobalt, the correlation coefficient is ρ = -0.77 ± 0.15. If the Greenstein (1949) hypothesis can explain the values of the correlation coefficients found by Yushchenko et al. (2015), it is possible to conclude that RM_1-390 has some significant convective energy transfer in its atmosphere.

It is to be noted that the Greenstein (1949) hypothesis was mentioned to explain the peculiar abundances in binary stars (Kang et al. 2012, 2013; Jeong et al. 2017). It was shown that the correlations between relative abundances and second ionization potentials of corresponding elements were observed not only in radiative atmospheres, but also in convective atmospheres in the case of strong flux accreted from the circumstellar envelope.

It is also necessary to mention a possible detection of Thorne-Żytkow objects (Thorne & Żytkow 1975). These objects have a massive nondegenerate envelope surrounding a degenerate neutron core. It can be the result of a strong accretion process onto an existing neutron star. These objects should have effective temperatures similar to those of red supergiants and their radii near 103 solar value. The observational properties of Thorne-Żytkow objects are very close to the properties of red supergiants, as such it is very difficult to identify such objects. Only few candidates have been discovered thus far (Levesque et al. 2014). Thorne-Żytkow objects should show strong lithium and some heavy elements lines in their spectra. The abundance pattern of RM_1-390 rejects this possibility as the relative abundances

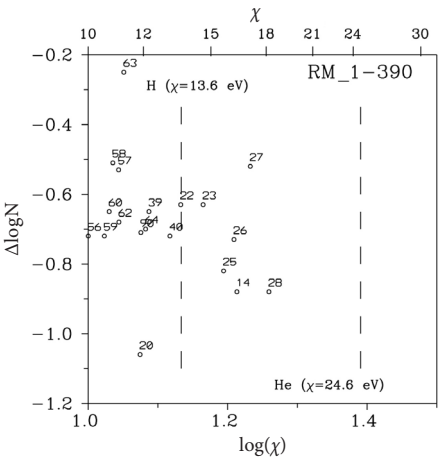

Fig. 4. The plot shows the relative surface abundances of chemical elements in the atmosphere of RM_1-390 as a function of second ionization potentials of these elements. The chemical elements are indicated by their atomic numbers. The ionization energies of hydrogen and helium are shown by the vertical dashed lines.

of yttrium and zirconium are of the same order as that of iron.

We can conclude that RM_1-390 has unusual colors, strong infrared excess and, possibly, variable radial velocities. The absorption lines of the both s- and r-process elements are detected in its spectrum. The abundance pattern can be fitted to the solar system s-process curve. The atmosphere of RM_1-390 shows signs of accretion of interstellar gas. The signs of some important convective energy transfer are detected in the atmosphere of this supergiant. All these features are consistent with the possible existence of a binary satellite and the strong circumstellar envelope.

ACKNOWLEDGMENTS

This work was supported in part by the Korea Astronomy and Space Science Institute under the R&D program (Project No. 2015-1-320-18) supervised by the Ministry of Science, ICT and Future Planning. One of the authors (V. Yu) was provided a grant by the Swiss National Science Foundation (SCOPES project No.~IZ73Z0152485).

REFERENCES

Adams SM, Kochanek CS, Gerke JR, Stanek, KZ, The search for failed supernovae with the Large Binocular Telescope: constraints from 7 yr of data, Mon. Not. R. Astron. Soc. 469, 1445-1455 (2017a). https://doi.org/10.1093/mnras/stx898

Adams SM, Kochanek CS, Gerke JR, Stanek KZ, Dai X, The search for failed supernovae with the Large Binocular

Telescope: confirmation of a disappearing star, Mon. Not. R. Astron. Soc. 468, 4968-4981 (2017b). https://doi.org/10.1093/mnras/stx816

Ardeberg A, Virdefors, B, Solar line blocking for λλ4006-6860, Astron. Astrophys. Suppl. Ser. 36, 317-321 (1979).

Biémont E, Palmeri P, Quinet P, Database on Rare Earths At Mons University (DREAM), [Internet], cited 2017 Apr 14, available from: http://hosting.umons.ac.be/html/agif/databases/dream.html

Bonanos AZ, Massa DL, Sewilo M, Lennon DJ, Panagia N, et al., *Spitzer* SAGE infrared photometry of massive stars in the Large Magellanic Cloud, Astron. J. 138, 1003-1021 (2009). https://doi.org/10.1088/0004-6256/138/4/1003

Bonanos AZ, Lennon DJ, Köhlinger F, van Loon JT, Massa DL, et al., *Spitzer* SAGE-SMC infrared photometry of massive stars in the Small Magellanic Cloud, Astron. J. 140, 416-429 (2010). https://doi.org/10.1088/0004-6256/140/2/416

Boyer ML, Srinivasan S, van Loon JT, McDonald I, Meixner M, et al., Surveying the agents of galaxy evolution in the Tidally Stripped, Low Metallicity Small Magellanic Cloud (SAGE-SMC). II. Cool evolved stars, Astron. J. 142, A103 (2011). https://doi.org/10.1088/0004-6256/142/4/103

Choudhury S, Subramaniam A, Cole AA, Photometric metallicity map of the Large Magellanic Cloud, Mon. Not. R. Astron. Soc. 455, 1855-1880 (2016). https://doi.org/10.1093/mnras/stv2414

Delbouille L, Roland G, Neven L, Photometric atlas of the solar spectrum from λ 3000 to λ 10000, special volume (University of Liège, Liège, 1973).

Elias JH, Frogel JA, Humphreys RA, M supergiants in the Milky Way and the Magellanic Clouds: colors, spectral types, and luminosities, Astrophys. J. Suppl. Ser. 57, 91-131 (1985). https://doi.org/10.1086/190997

Fuhr JR, Wiese WL, A critical compilation of atomic transition probabilities for neutral and singly ionized iron, J. Phys. Chem. Ref. Data 35, 1669-1809 (2006). https://doi.org/10.1063/1.2218876

González-Fernández C, Dorda R, Negueruela I, Marco A, A new survey of cool supergiants in the Magellanic Clouds, Astron. Astrophys. 578, A3 (2015). https://doi.org/10.1051/0004-6361/201425362

Gopka VF, Yushchenko AV, Mishenina TV, Kim C, Musaev FA, et al., Atmospheric chemical composition of the halo star HD 221170 from a synthetic-spectrum analysis, Astron. Rep. 48, 577-587 (2004). https://doi.org/10.1134/1.1777275

Gopka VF, Shavrina A, Vasileva S, Yushchenko A, Andrievsky S, et al., Preliminary study of red supergiant RM_1-667 in the Large Magellanic Cloud, Odessa Astron. Publ. 25, 64-65 (2012a).

Gopka VF, Shavrina AV, Vasilyeva SV, Andrievsky SM, About chemical composition of supergiant PMMR145 in Small Magellanic Cloud. Osmium, Odessa Astron. Publ. 25, 167-168 (2012b).

Gopka VF, Shavrina AV, Yushchenko VA, Vasil'eva SV, Yushchenko AV, et al., On the thorium absorption lines in the visible spectra of supergiant stars in the Magellanic Clouds, Bull. Crime. Astrophys. Obs. 109, 41-47 (2013a). https://doi.org/10.3103/S0190271713010087

Gopka VF, Yushchenko A, Kovtyukh V, Shavrina A, Yushchenko V, et al., The abundances of heavy elements in red supergiants of Magellanic Clouds, Odessa Astron. Publ. 26, 54-59 (2013b).

Greenstein JL, Analysis of the Metallic-Line stars. II, Astrophys. J. 109, 121-138 (1949). https://doi.org/10.1086/145112

Grevesse N, Sauval AJ, The solar abundance of iron and the photospheric model, Astron. Astrophys. 347, 348-354 (1999).

Gustafsson B, Edvardsson B, Eriksson K, Mizuno-Wiedner M, Jørgensen UG, et al., A grid of model atmospheres for cool stars, ASP Conference Series, vol. 288, Stellar Atmosphere Modeling, eds. Hubeny I, Mihalas D, Werner K (Astronomical Society of the Pacific, San Francisco, 2003), 331-334.

Hill V, Chemical composition of six K supergiants in the Small Magellanic Cloud, Astron. Astrophys. 324, 435-448 (1997).

Hirata R, Horaguchi T, VizieR online data catalog: atomic spectral line list, SIMBAD catalog VI/69 (1995). available from: http://vizier.cfa.harvard.edu/viz-bin/Cat?VI/69

Humphreys RM, M supergiants and the low metal abundances in the Small Magellanic Cloud, Astrophys. J. 231, 384-387 (1979). https://doi.org/10.1086/157201

Jeong Y, Yushchenko AV, Doikov DN, Gopka VF, Yushchenko VO, Chemical composition of RR Lyn – an eclipsing binary system with Am and λ Boo type components, J. Astron. Space Sci. 34, 75-82 (2017). https://doi.org/10.5140/JASS.2017.34.2.75

Kang YW, Yushchenko A, Hong K, Kim S, Yushchenko V, Chemical composition of the components of eclipsing binary star ZZ Bootis, Astron. J. 144, A35 (2012). https://doi.org/10.1088/0004-6256/144/2/35

Kang YW, Yushchenko AV, Hong K, Guinan EF, Gopka VF, Signs of accretion in the abundance patterns of the components of the RS CVn-type eclipsing binary star LX Persei, Astron. J. 145, A167 (2013). https://doi.org/10.1088/0004-6256/145/6/167

Kochanek CS, Beacom JF, Kistler MD, Prieto JL, Stanek KZ, et al., A survey about nothing: monitoring a million supergiants for failed supernovae, Astrophys. J. 684, 1336-1342 (2008). https://doi.org/10.1086/590053

Kurucz RL, SYNTHE spectrum synthesis programs and line data,

Kurucz CD-ROM (Smithsonian Astrophysical Observatory, Cambridge, 1993).

Levesque EM, Massey P, Żytkow AN, Morrell N, Discovery of a Thorne-Żytkow object candidate in the Small Magellanic Cloud, Mon. Not. R. Astron. Soc. Lett. 443, L94-L98 (2014). https://doi.org/10.1093/mnrasl/slu080

Massey P, Olsen KAG, The evolution of massive stars. I. Red supergiants in the Magellanic Clouds, Astron. J. 126, 2867-2886 (2003). https://doi.org/10.1086/379558

Morton DC, Atomic data for resonance absorption lines. II. Wavelengths longward of the Lyman limit for heavy elements, Astrophys. J. Suppl. Ser. 130, 403-436 (2000). https://doi.org/10.1086/317349

Munari U, Henden A, Frigo A, Zwitter T, Bienaymé O, et al., APASS Landolt-Sloan *BVgri* photometry of RAVE stars. I. Data, effective temperatures, and reddening, Astron. J. 148, A81 (2014). https://doi.org/10.1088/0004-6256/148/5/81

Piskunov NE, Kupka F, Ryabchikova TA, Weiss WW, Jeffery CS, VALD: the Vienna atomic line data base, Astron. Astrophys. Suppl. Ser. 112, 525-535 (1995).

Rutten RJ, van der Zalm EBJ, Revision of solar equivalent widths, Fe I oscillator strengths and the solar iron abundance, Astron. Astrophys. Suppl. Ser. 55, 143-161 (1984).

Simmerer J, Sneden C, Cowan JJ, Collier J, Woolf VM, et al., The rise of the s-process in the Galaxy, Astrophys. J. 617, 1091-1114 (2004). https://doi.org/10.1086/424504

Szczygieł DM, Stanek KZ, Bonanos AZ, Pojmański G, Pilecki B, et al., Variability of luminous stars in the Large Magellanic Cloud using 10 years of ASAS data, Astron. J. 140, 14-24 (2010). https://doi.org/10.1088/0004-6256/140/1/14

Thorne KS, Żytkow AN, Red giants and supergiants with degenerate neutron cores, Astrophys. J. 199, L19-L24 (1975). https://doi.org/10.1086/181839

Yushchenko AV, URAN: a software system for the analysis of stellar spectra, Proceedings of the 20th Stellar Conference of the Czech and Slovak Astronomical Institutes, ed. Dusek J (the Czech and Slovak Astronomical Institutes, Brno, 1998), 201-203.

Yushchenko AV, Gopka VF, Khokhlova VL, Musaev FA, Bikmaev IF, Atmospheric chemical composition of the "twin" components of equal mass in the CP SB2 system 66 Eri, Astron. Lett. 25, 453-466 (1999).

Yushchenko AV, Gopka VF, Kang YW, Kim C, Lee, BC, et al., The chemical composition of ρ Puppis and the signs of accretion in the atmospheres of B-F-type stars, Astron. J. 149, A59 (2015). https://doi.org/10.1088/0004-6256/149/2/59